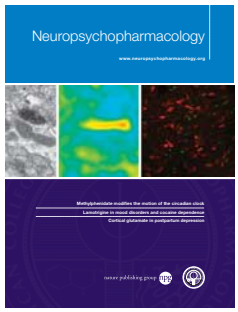

A Key Role for Neurotensin in Chronic-Stress-Induced Anxiety-Like Behaviour in Rats

Catherine P Normandeau, Ana Paula Ventura Silva, Emily R Hawken, Staci Angelis, Calvin Sjaarda, Xudong Liu, José Miguel Pêgo, Éric C Dumont

Cite this article as: Catherine P Normandeau, Ana Paula Ventura Silva, Emily R Hawken, Staci Angelis, Calvin Sjaarda, Xudong Liu, José Miguel Pêgo, Éric C Dumont, A Key Role for Neurotensin in Chronic-Stress-Induced Anxiety-Like Behaviour in Rats, *Neuropsychopharmacology* accepted article preview 26 June 2017; doi: 10.1038/npp.2017.134.

Received 21 April 2017; revised 15 June 2017; accepted 16 June 2017; Accepted article preview online 26 June 2017

Title: A key role for neurotensin in chronic-stress-induced anxiety-like behaviour in rats

Running Title: Neurotensin and anxiety-like behaviours

Catherine P. Normandeau[1], Ana Paula Ventura Silva[2,3], Emily R. Hawken[1], Staci Angelis[1], Calvin Sjaarda[4], Xudong Liu[4], José Miguel Pêgo[2,3], Éric C. Dumont[1]

[1]Center for Neuroscience Studies and Department of Biomedical and Molecular Sciences, Queen's University, Kingston, Ontario, Canada

[2]Life and Health Sciences Research Institute (ICVS), School of Medicine Sciences, University of Minho, Braga, Portugal

[3]ICVS/3B's—PT Government Associate Laboratory, Braga/Guimarães, Portugal

[4]Queen's Genomics Lab at Ongwanada (QGLO), Queen's University, Kingston, Ontario, Canada

Corresponding Author Information: Correspondence and requests for materials should be addressed to:

Éric C. Dumont
116 Barrie St
Biosciences Complex Room 1445
Kingston, ON, Canada
K7L 3N6
Email: eric.dumont@queensu.ca
Phone: 613-533-6991

Abstract

Chronic stress is a major cause of anxiety disorders that can be reliably modeled pre-clinically, providing insight into alternative therapeutic targets for this mental health illness. Neuropeptides have been targeted in the past to no avail possibly due to our lack of understanding of their role in pathological models. In this study we use a rat model of chronic stress-induced anxiety-like behaviours and hypothesized that neuropeptidergic modulation of synaptic transmission would be altered in the Bed Nucleus of the Stria Terminalis (BNST), a brain region suspected to contribute to anxiety disorders. We use brain slice neurophysiology and behavioural pharmacology to compare the role of locally released endogenous neuropeptides on synaptic transmission in the oval (ov) BNST of non-stressed (NS) or chronic unpredictably stressed (CUS) rats. We found that in NS rats, post-synaptic depolarization induced the release of vesicular neurotensin (NT) and corticotropin releasing factor (CRF) that co-acted to increase ovBNST inhibitory synaptic transmission in 59% of recorded neurons. CUS bolstered this potentiation (100% of recorded neurons) through an enhanced contribution of NT over CRF. In contrast, locally-released opioid neuropeptides decreased ovBNST excitatory synaptic transmission in all recorded neurons, regardless of stress. Consistent with CUS-induced enhanced modulatory effects of NT, blockade of ovBNST neurotensin receptors completely abolished stress-induced anxiety-like behaviours in the elevated plus maze paradigm. The role of NT has been largely unexplored in stress and our findings highlight its potential contribution to an important behavioural consequence of chronic stress, that is, exaggerated avoidance of open space in rats.

Introduction

While the stress response is integral for survival, prolonged exposure to stressors can have damaging consequences. Repeated exposure to aversive stressors predicts and contributes to mental illnesses such as generalized anxiety disorders (GAD), major depressive disorder (MDD), or post-traumatic stress disorder (PTSD) (Deppermann *et al*, 2014; Gosselin and Laberge, 2003; Hammen *et al*, 2009). However, the biochemical imbalances caused by repeated stress in the brain remain elusive and animal models of chronic stress are essential to elucidate these mechanisms (Conrad *et al*, 2011).

Repeated aversive stressors result in increased volume and dendritic branching as well as long-term alterations of excitatory synaptic transmission in the bed nucleus of the stria terminalis (BNST) (Conrad *et al*, 2011; Dabrowska *et al*, 2013; Glangetas *et al*, 2013; Hubert and Muly, 2014; McElligott *et al*, 2010; Pego *et al*, 2008; Vyas *et al*, 2003). Surprisingly, the effects of chronic stress on local γ-aminobutyric acid (GABA) transmission, imperative for fine-tuning neuronal output, have been largely unexplored in the BNST. Neuropeptides are potent modulators of GABA transmission in the BNST, but whether their function is altered in chronically stressed rats has never been investigated (Crowley *et al*, 2016; Kash and Winder, 2006; Krawczyk *et al*, 2013). Neuropeptides in the BNST may be affected by chronic stress due to their involvement in the modulation of stress- or aversion-related phenomena (Lezak *et al*, 2014; Walker *et al*, 2009).

Specifically, the oval nucleus of the BNST (ovBNST) contains high concentrations of many different neuropeptides and activation of this specific

nucleus increases anxiety-like behaviours suggesting it may be sensitive to chronic stress (Kim *et al*, 2013). Therefore, we hypothesized that chronic stress would change neuropeptide modulation of synaptic transmission in the ovBNST. We used the chronic unpredictable stress (CUS) paradigm to test this hypothesis, a preclinical model that mimics every day stressors and invariably increases anxiety-like behaviours in rats (Cerqueira *et al*, 2007). Interestingly, the neuromodulatory effects of neurotensin (NT), but not of corticotropin releasing factor (CRF), became sensitized after one-month exposure to CUS. Accordingly, *in vivo* pharmacological blockade of ovBNST NT receptors had an anxiolytic effect in CUS rats. The neuropeptide NT is therefore a significant contributor to ovBNST promotion of anxiety-like behaviour in chronically stressed animals.

Methods and Materials

Rats

One hundred and thirty-three adult male rats (Charles River Laboratories, Canada/Spain) weighing 350-450g were included in the electrophysiology experiments (Wistar and Long Evans rats, n=63) and behavioural experiments (Wistar rats, n=70). The rats were maintained on an artificial 12h light/dark cycle (8:00 A.M. lights on/8:00 P.M. lights off) or 12h dark/light cycle (8:00 A.M. lights off/8:00 P.M. lights on).

The rats acclimatized for a minimum of 1 week upon arrival to the facility. Rat chow and water were provided *ad libitum* in the home cages. Sixty-three rats were used for electrophysiology (Canada), 33 rats performed the elevated plus

maze (Portugal), and 37 rats performed the elevated plus maze and the forced swim test (Canada). All experiments were conducted in accordance with the guidelines from the Canadian Council on Animal Care in Science and approved by the Queen's University Animal Care Committee and with Portugal local regulations (European Union Directive 86/609/EEC).

Slices preparation and electrophysiology

Rats were anesthetized with isoflurane (5% at 5 L/min) and their brains removed into ice-cold artificial cerebral spinal fluid (aCSF) containing (in mM): 126 NaCl, 2.5 KCl, 1.2 $MgCl_2$, 6 $CaCl_2$, 1.2 $NaH2PO_4$, 25 $NaHCO_3$, and 12.5 D-glucose equilibrated with 95% O_2/5% CO2. Brains were cut in 2°C aCSF into coronal slices (250 μm) with a vibrating blade microtome (VT-1000; Leica). We used the slice corresponding to -0.26mm from bregma. Slices were incubated at 34°C for 60 minutes and transferred to a chamber perfused (3 ml/min) with aCSF at 34°C. Remaining slices were kept in aCSF at room temperature until further use. Whole-cell voltage-clamp recordings were made using glass microelectrodes (3-5 MΩ) filled with (in mM): 70 K+-gluconate, 80 KCl, 1 EGTA, 5 HEPES, 2 MgATP, 0.3 GTP, and 1 P-creatine. We recorded lateral from an imaginary line drawn vertically across the lateral ventricle and medial to the internal capsule. In the dorso-ventral plan, we only recorded dorsally to an imaginary horizontal line drawn half-way between the ventral tip of the lateral ventricle and the top of the anterior commissure as illustrated in our previous publications (Krawczyk *et al*, 2011a; Krawczyk *et al*, 2011b). Paired electrical stimuli (10–100 μA, 0.1 ms duration, 20 Hz) were applied at 0.1 Hz. Excitatory or inhibitory post-synaptic currents

(E/IPSCs) were evoked by local fiber stimulation with tungsten bipolar electrodes while neurons were voltage-clamped at −70 mV. $GABA_A$-IPSC and AMPA-EPSC were pharmacologically isolated with 6,7-dinitroquinoxaline-2,3-dione (DNQX; 50 μM) or picrotoxin (100μM), respectively. To induce local endogenous neuropeptide release, post-synaptic neurons were repetitively depolarized in voltage clamp from -70 to 0 mV (100 ms) at a frequency of 2 Hz for 5 mins (Iremonger and Bains, 2009).

We defined long-lasting post-synaptic depolarization-induced changes in E or IPSCs peak amplitude as a >20% deviation from baseline, 25 mins following the end of the repetitive depolarization protocol. Recordings were made using a Multiclamp 700B amplifier and a Digidata 1440A (Molecular Devices Scientific). Data were acquired and analyzed with Axograph X running on Apple computers.

Drugs

Stock solutions of SR 142948 (10 mM) and naloxone (1 mM) were prepared in double-distilled water and stock solutions of DNQX (100 mM), NBI-27914 (50 mM), Concanamycin A (1mM) were prepared in DMSO (100%). All drugs were further dissolved in the physiological solutions or 0.9% saline at the desired concentrations (DNQX 50μM, SR-142948 5-10 μM, NBI-27914 1 μM, Concanamycin A 5 μM, naloxone 1 μM) and the final DMSO concentration never exceeded 0.1%. Drugs were obtained from Sigma-Aldrich or R&D Systems.

Chronic Unpredictable Stress (CUS)

Rats were singly-housed and randomly assigned to non-stressed (NS) or CUS groups. Rats in the NS group were handled regularly over 4 weeks. Rats in the CUS group were exposed to 4 weeks of daily exposure to one stressor (10-60 min/day)

at different times, as described previously (Cerqueira *et al*, 2007). Stressors presentation was randomized and included one of the following aversive stimuli: cold water immersion (18°C, 60 mins), home cage shaking (10 mins), restraining (60 mins), overcrowding (3-4 rats/cage, 60 mins), and exposure to hot air stream (15 mins).

Surgery

Rats were positioned in a stereotaxic instrument and secured by non-rupture ear bars under isoflurane (2-3%, 5L/min) or ketamine/medetomidine anaesthesia. Double guide cannulas (Plastics One) were bilaterally implanted 1 mm above the upper limit of the oval region of the dorsal BNST (−0.26 A.P., ±1.9 M.L., −6.5 D.V.). Injector cannulas (Plastics One) were placed into the guide cannulas (7.5 mm length). All stereotaxic coordinates were relative to bregma. The head attachment was secured in place via four 0.08 × 0.125 in jeweler screws and dental acrylic cement. The guide cannulas were fitted with an autoclaved 30 Ga stylet and covered with a screw-on dust cap. Following surgery, the rats recovered for one week and then were randomly assigned to six experimental groups: NS (saline, n=11); NS SR 5 (SR-142948 5 μM, n=8), NS SR 10 (SR-142948 10 μM, n=6), CUS saline (saline, n=16), CUS SR 5 (SR-142948 5 μM, n=12) and CUS SR 10 (SR 142948 10 μM, n=17). Three rats (2 in the NS SR5 group and 1 in the NS SR 10 group) were euthanized before the forced swim test due to health issues.

Behavioural Tests

The rats were placed in the NS groups or the CUS groups receiving a 300nL injection of either saline, SR-142948 5 μM, or SR-142948 10 μM 30 mins before

testing (Binder *et al*, 2001). Behavioural testing was done on 3 consecutive days, starting with the elevated-plus maze (EPM) followed by the forced swim test (FST).

Elevated Plus Maze (EPM)

Rats were tested for 5 mins in the EPM using a black polypropylene "plus"-shaped maze (Med Associates) as previously described (Pego *et al*, 2008). The maze consisted of two facing open arms (50.8 x 10.2 cm) and two closed arms (50.8 x10.2 x 40.6 cm), 72 cm above the floor. Testing was performed under bright white light (≅ 40 lux). The time spent in the open arms, junction area and closed arms, as well as the number of entrances and explorations in each section were recorded using a system of infrared photo beams, the crossings of which were monitored by a computer. The times spent in each of the compartments of the EPM are presented as percentage of the total duration of the trial.

Forced Swim Test (FST)

Rats were introduced to a cylindrical container filled with 30 cm of water (23-25°C) for 15 minutes during pre-test and 5 mins during testing. The rats' behaviour was categorized as 1) immobile, 2) swimming and 3) climbing (included diving). We defined immobile as the absence of directed movements, climbing as vertical movement of the forepaws and swimming as horizontal movement in the swim chamber. The predominant behaviour over each 5-sec period of the 300-sec test was rated over a total score of 60 by an experimenter blind to the pharmacological treatment or the stress group.

Open Field

Animals were individually tested for 5 min each in an open field (OF) arena (43.2 ×

43.2 cm) that had transparent acrylic walls and a white floor (model ENV-515, MedAssociates Inc, St. Albans, VT 05478). Each subject was initially placed in the center of the arena and horizontal activity and instant position were registered, using a system of two 16-beam infrared arrays connected to a computer. Total distances were used as indicators of locomotor activity.

Histological Procedures

Following behavioural testing, the rats were anaesthetized with pentobarbital or isoflurane. Extracted brains were submerged in fresh paraformaldehyde for 2 days and switched to 30% sucrose paraformaldehyde for cryoprotection. The brains were kept at −80°C until histology. Thirty µm coronal sections were sliced and stained with cresyl violet to assess the location of the central injections (Figure 5B,C).

RNA extraction and reverse transcription

Brain sections containing the dorsal BNST or the central amygdala (Figure S1) were collected from RNAlater (ThermoFisher Scientific) solution with a sterile tissue puncher and submerged in 100 uL of lysis/binding buffer from the Dynabeads mRNA Direct Micro Kit (ThermoFisher Scientific). The tissue was immediately homogenized in microcentrifuge tubes using a disposable pestle (Fisherbrand). mRNA was purified using the Dynabeads mRNA Direct Micro Kit (ThermoFisher Scientific) following the manufacturer's recommended protocol for mRNA isolation from tissues. mRNA concentration was determined using the Qubit Fluorometer 2.0 (ThermoFisher Scientific). 40 ng of mRNA from each sample was reverse transcribed using the SuperScript IV First-Strand Synthesis kit (Invitrogen) in an

Applied Biosystems GeneAmp PCR System 9700 (ThermoFisher Scientific).

Real time qPCR and data analysis

The cDNA was amplified in the ViiA7 Real-Time PCR machine (ThermoFisher Scientific) with a two-step PCR protocol (95°C for 10 minutes followed by 40 cycles of 95°C for 15 seconds and 60°C for 1 minute) using the Power SYBR Green PCR Master Mix (ThermoFisher Scientific) and KiCqStart SYBR Green Primers (Sigma-Aldrich) (Table S1). Each reaction was performed in triplicate and dissociation curves were generated for all reactions to ensure primer specificity. All target genes were normalized to 3 reference genes (*Sdha*, *Actb* and *Hprt*) and the relative quantification using the comparative Ct method was determined using the DataAssist Software Version 3.01 (ThermoFisher Scientific).

Statistical analyses

Changes in E/IPSCs peak amplitude were measured from baseline and are shown as percentages as follows: (Peak amplitude$_{post}$–Peak amplitude$_{baseline}$/Peak amplitude$_{baseline}$)*100. Data are reported as means ± SEM and each data point represents the average of values in 1 min bins (6 evoked E/IPSCs) across recorded neurons.

Two-way ANOVAs were used to compare multiple means of parametric data and Kruskal-Wallis H Test for non-parametric. A Bonferroni correction was used for multiple comparisons. Mann Whitney U test was used to compare specific means with an adjusted p-value according to the number of test performed. Fisher's exact tests and Chi Squares analyzed contingency tables of the neuronal response distribution. All statistical analyses were done with SPSS Statistics Version 23 (SAS

Institute) or Prism 6.

Results

Post-synaptic activation of ovBNST neurons (0mV, 100msec, 2Hz, 5 mins) resulted in robust long-lasting depolarization-induced enhancement of inhibition (l-DEI) in 59% of recorded neurons (time x group, $F_{1,32}$=7.9, P<0.0001, n=20/34 cells l-DEI from 21 rats; Figure 1A,F). The addition of the v-ATPase inhibitor concanamycin A (5μM) to the intracellular recording solution completely ablated ovBNST l-DEI that was thus vesicular release-dependent (Fisher's Exact Test (NS-aCSF vs. NS-Conc), P=0.04, n=0/4 cells l-DEI from 2 rats; Figure 1B,F). Additionally, rat strain and light cycle had no effect on l-DEI cell response ($X^2_{(2,n=34)}$=4.69, P=0.1; Table S2).

The ovBNST is exclusively populated with GABA neurons that also contain the neuropeptides NT, CRF, dynorphin, or enkephalin (Day *et al*, 1999; Ju *et al*, 1989b; Poulin *et al*, 2009). NT and CRF both increase ovBNST $GABA_A$-inhibitory post-synaptic currents (IPSCs) through either NT receptors (NTR) or CRF receptors 1 (CRFR1), respectively, and we hypothesized that one or both could be responsible for l-DEI (Kash *et al*, 2006; Krawczyk *et al*, 2013). As such we used a non-selective NTR antagonist (SR-142948, 10μM) and a CRFR1 selective antagonist (NBI-27914, 1μM). Blocking NTR did not significantly block l-DEI (Fisher's Exact Test (NS-aCSF vs. NS-SR), P=0.1, n=6/18 cells l-DEI from 11 rats; Figure 1C,F). Likewise, l-DEI was unaltered (56% of neurons) by the CRF antagonist (Fisher's Exact Test (NS-aCSF vs. NS-NBI), P=1.0, n=5/9 cells l-DEI from 6 rats; Figure 1D,F). However, co-application of SR-142948 and NBI-27914 completely eliminated l-DEI indicating cooperation between NT and CRF in producing l-DEI, which is consistent with their co-

localization in ovBNST neurons (Fisher's Exact Test (NS-aCSF vs. NS-SR/NBI), P=0.004, n=0/8 cells l-DEI from 4 rats; Figure 1E,F)(Ju and Han, 1989a). Interestingly, bath application of NTR antagonist but not CRFR1 antagonist resulted in a reversible depression of $GABA_A$-IPSCs suggesting constitutive NTR activity (Figure S2). Additionally, neither NT bath application or repetitive depolarization changed holding current or input resistance indicating membrane potential and channels were not changed by the neuropeptide (Table S3).

We next determined whether l-DEI might be altered in the ovBNST of chronically stressed rats. CUS significantly facilitated l-DEI (Time, $F_{1,10}$=5.0, P=0.009, n=11/11 cells l-DEI from 7 animals; Figure 2A) that was now measurable in all tested neurons compared to the NS group ($X^2_{(1,n=45)}$=6.6, P=0.01; Figure 2E). The NTR antagonist significantly reversed CUS-induced facilitation of l-DEI suggesting that NT took over modulation of ovBNST inhibitory synaptic transmission in stressed conditions (Fisher's Exact Test (CUS-aCSF vs. CUS-SR), P=0.0002, n=2/10 cells l-DEI from 4 rats, Figure 2B,E). In contrast, CRFR1 blockade had no effect on l-DEI in CUS rats (Fisher's Exact Test (CUS-aCSF vs. CUS-NBI), P=1.0, n=11/12 cells l-DEI from 3 rats, Figure 2C,E) although both CRF and NT antagonists were necessary to completely eliminate l-DEI (Fisher's Exact Test (CUS-aCSF vs. CUS-SR/NBI), P=0.0001, n=0/8 cells l-DEI from 5 rats, Figure 2D,E).

We then investigated changes in mRNA expression of CRF, NT and their receptors in the dorsal BNST (dBNST) and, the central amygdala (CeA) that has strong inhibitory inputs onto the ovBNST and a similar neuropeptide array (expressing both CRF and NT) (Day *et al*, 1999). In support of CUS-induced changes

in the NT system, CUS significantly and selectively reduced dBNST *Ntsr1* mRNA levels compared to NS (P=0.05, Figure 2F). In contrast, CUS had no significant effect on other stress-related transcripts in either the dBNST or the CeA (Figure 2F,G).

In NS animals, post-synaptic depolarization resulted in long-lasting depolarization-induced reduction of excitatory synaptic transmission (l-DRE) in all tested neurons (time, $F_{1,7}$=12.2, P<0.0001, n=9/9 cells l-DRE from 6 rats; Figure 3A,C). The broad-spectrum opioid receptor antagonist naloxone (Nal, 10μM) abolished l-DRE suggesting that post-synaptic depolarization triggered the local release of endogenous opioids (Fisher's Exact Test (NS-aCSF vs. NS-Nal), P=0.002, n=2/9 cells l-DRE from 4 rats, Figure 3B,C). The effect of post-synaptic activity on excitatory transmission was largely unaffected by CUS and still resulted in robust l-DRE in the vast majority of recorded ovBNST neurons (time, $F_{1,5}$=4.2, P=0.05, n=6/7 cells l-DRE from 3 rats; Fisher's Exact Test (NS vs. CUS), P=0.4, Figure 4A,C). Similar to NS conditions, Nal completely blocked l-DRE (Figure 4B), supporting the involvement of locally released endogenous opioids in this response (Fisher's Exact Test (CUS-aCSF vs. CUS-Nal), P= 0.005, n=0/6 cells l-DRE from 3 rats, Figure 4C).

CUS increases avoidance of open arms in the elevated plus maze (EPM) and immobilization in the forced swim test (FST) (Bessa *et al*, 2009). Converging evidence suggests that the BNST plays a key role in these chronic stress-induced anxiety- and depression-like phenomena (Daniel and Rainnie, 2016). Since CUS altered the neuromodulatory effect of NT in the ovBNST, we hypothesized that *in vivo* pharmacological blockade of ovBNST NTR might reverse CUS-induced avoidance of open arms in the EPM and immobility in the FST. As expected, CUS

significantly reduced the percentage of time spent in the open arms in saline-treated rats (U=5, p=0.0002, Figure 5D). Intra-ovBNST SR-142948 (5-10μM/side) had no effect on EPM behaviours in NS but significantly increased the percentage of time spent in the open arms in CUS (Kruskal-Wallis H test, X^2_5=18.2, P=0.003, Figure 5D). SR-142948 (5-10μM/side) dose-dependently reversed this effect in CUS rats (U=7, P=0.0001, Figure 5D). SR-142948 had no effect on the number of open arms entries (Kruskal-Wallis H test, X^2_5=5.3, P=0.4, Figure 5E) and did not affect total distance travelled in the open field ($F_{(3,32)}$=0.7, p=0.6, Figure S3) therefore did not affect locomotion. In our conditions, intra-ovBNST NTRs blockade had no effect on immobility scores in the FST in either NS or CUS conditions (Kruskal-Wallis H test, X^2_5=8.6, P=0.1, Figure 5F).

Discussion

We used brain slice whole-cell voltage-clamp recordings and discovered that in the ovBNST of NS rats, post-synaptic activation resulted in long-lasting depolarization-induced enhancement of inhibitory $GABA_A$- and reduction of excitatory AMPA synaptic transmission that we termed l-DEI and l-DRE, respectively. NT and CRF both produced l-DEI while opioids were fully responsible for l-DRE. CUS facilitated l-DEI through an enhanced contribution of NT whereas l-DRE was not affected. Pharmacological blockade of ovBNST NT receptors abolished CUS-induced reduction in open arm avoidance in the elevated plus maze, suggesting that NT may contribute to anxiety disorders (Laszlo *et al*, 2010; Saiz Ruiz *et al*, 1992).

In NS rats, post-synaptic activation produced l-DEI in slightly over half (59%) of recorded ovBNST neurons. There is clear evidence of various ovBNST neurons subpopulations with distinct morphological, neurochemical, or electrophysiological signatures that could explain this dichotomy (Day *et al*, 1999; Hammack *et al*, 2007; Ju *et al*, 1989b; Larriva-Sahd, 2006; Poulin *et al*, 2009). The neuron-specific expression of l-DEI may be tightly linked with specific neuropeptidergic profiles (Iremonger *et al*, 2009; Ludwig and Pittman, 2003). NT and CRF are highly concentrated in ovBNST neurons and both neuropeptides robustly potentiate $GABA_A$-mediated synaptic transmission although through distinct pre- and post-synaptic loci, respectively (Day *et al*, 1999; Ju *et al*, 1989a; Kash *et al*, 2006; Krawczyk *et al*, 2013). A study combining brain slice electrophysiology and single-cell PCR showed that 60% of ovBNST neurons contain CRF which is precisely the percentage of l-DEI response we obtained, supporting a role for CRF in l-DEI (Dabrowska *et al*, 2011). Importantly, CRF and NT co-localize in the ovBNST and pharmacological blockade of both CRFR1 and NTR was necessary to completely abolish l-DEI (Ju *et al*, 1989a). Application of either neuropeptide antagonist alone did not block l-DEI suggesting a cooperative mechanism where one neuropeptide activity can compensate for the blockage of the other. The exact functional link however remains elusive.

Post-synaptic activation also resulted in opioid-dependent l-DRE in all recorded ovBNST neurons in NS rats, mitigating the possibility of sub-population effects. Only 41% of ovBNST neurons seem to express detectable amounts of enkephalins mRNA which poorly co-localizes with CRF or NT (Day *et al*, 1999).

Dynorphin is also abundant in the rat ovBNST and may have contributed to the opioid-dependent l-DRE we measured (Poulin *et al*, 2009). Enkephalin and dynorphin are potent inhibitors of excitatory synaptic transmission in the brain, supporting opioid-dependent l-DRE (Crowley *et al*, 2016). Opioid neuropeptides also modulate inhibitory transmission but we did not detect this response likely due to their short-lasting effects that we did not include in our analyses (Crowley *et al*, 2016; Dumont and Williams, 2004).

Altogether, our data show that blocking CRFR1, NTR, and opioid receptors completely abolished post-synaptic activation-induced modulation of synaptic transmission in the rat ovBNST. This does not preclude that other stimulation patterns may trigger local synthesis and/or release of other neuromodulators (Puente *et al*, 2010) or of other neuropeptides expressed in ovBNST neurons (Woodhams *et al*, 1983). In addition, we focused on long-lasting changes in synaptic transmission but short-duration phenomena have also been reported (Puente *et al*, 2010). Unquestionably, numerous other neuropeptides, monoamines, or other molecules originating outside the ovBNST also robustly modulate synaptic transmission in this area (Dumont *et al*, 2004; Kash *et al*, 2006; Krawczyk *et al*, 2013; Krawczyk *et al*, 2011b; Li *et al*, 2012; McElligott and Winder, 2008; Shields *et al*, 2009). Nevertheless, the objective of the study was to determine whether local neuropeptidergic synaptic modulation was affected by chronic stress.

The neurophysiological mechanisms responsible for chronic stress-induced increase in anxiety-like behaviours are still largely unknown. Here, CUS facilitated l-DEI and NT was responsible for this effect whereas the contribution of CRF was

mitigated by stress. This is a novel observation considering that NT has been largely overlooked as a potential contributor in the pathological consequences of stress, compared to CRF (Saiz Ruiz *et al*, 1992). Alteration of NT function could be due to an increase in NT synthesis, release or receptor membrane expression, binding or coupling. Under normal physiological conditions, NT increases inhibitory transmission by binding pre-synaptically to NTRs in the ovBNST (Krawczyk *et al*, 2013). NT increases excitability and firing rate in other brains areas but we did not detect post-synaptic changes in the membrane potential or membrane channels opening suggesting these were not altered in the ovBNST (Jassar *et al*, 1999; Xiao *et al*, 2014)). Interestingly, the NTR receptor antagonist reversibly depressed $GABA_A$-IPSCs amplitude, in a seemingly inverse agonist way. The NTR2 exhibits constitutive activity on inositol phosphate production (Richard *et al*, 2001). Thus, the inverse agonist activity could occur through NTR2s that are also highly expressed in the BNST GABA neurons (Mazzone *et al*, 2016). However, it is still unknown whether the l-DEI is specific to or a combination of NTR1 and NTR2 activity and whether this is altered with CUS.

When we investigated mRNA expression, only *Ntsr1* mRNA, and not *Nts or Ntsr2*, was decreased in CUS rats compared to NS. Our findings corroborate other studies showing reduction of *Ntsr1* mRNA following maternal separation or CRF-overexpressing mice (Peeters *et al*, 2004; Toda *et al*, 2014). CUS decreasing *Ntsr1* mRNA expression may not result in a reduction of the NTR1 receptor expression at the cellular membrane. A decrease in *Ntsr1* mRNA could be due to an increase in mRNA stability or a compensatory mechanism to reduce increased NT activity. The

latter explanation could indicate that NTR1 expression is actually increased with CUS and may be responsible for the changes in cell responses. Future studies investigating protein level expression is necessary to fully understand the neurophysiological changes occurring with CUS.

The CUS paradigm in this study utilizes variable and uncontrollable stress where the animal does not habituate to the repeated stressors over time (Herman, 2013). As predicted from previous studies, we found that rats that underwent the CUS paradigm spent significantly less time in the open arms compared to their NS counterparts. Whether this behaviour is "adaptive" or "maladaptive" is unclear. In the context of our EPM test, chronically stressed animals could be mounting an adaptive response to a reasonably imminent threat. Alternatively, their response could be interpreted as maladaptive as the animal limits their exploration and possibility of finding resources in the absence of an immediate threat. Since the rats had no controllability over the stressors, it is impossible to distinguish whether they were mounting a contextually appropriate or inappropriate response.

Intra-ovBNST micro-injections of a NTR antagonist did however robustly modify CUS rats behaviours in the EPM, tying the sensitized NT neurophysiological response in ovBNST neurons of stressed rats with their anxiety profile. NTR blockade reversed the anxiogenic effect of CUS without affecting normal EPM exploratory behaviour displayed by NS rats. This is consistent with the fact that NT seems particularly important in mounting physiological and behavioural responses to face potentially extreme conditions (e.g. store fat, seek rich and highly rewarding nutrients, increase vigilance)(Deutch *et al*, 1987; Geisler *et al*, 2006; Krawczyk *et al*,

2013; Li *et al*, 2016; Luttinger *et al*, 1982). We also tested the effect of CUS on immobility in the FST but we did not find any changes in behaviour previously reported (Bessa *et al*, 2009). This discrepancy may be due to the shorter duration of the stress paradigm although our data showed that NT in the ovBNST may not contribute to this behaviour, regardless of the stress condition (Crestani *et al*, 2010).

Overall, these findings elucidate a clear role for NT in chronic stress although we cannot conclude exactly how NT-induced increase of GABA transmission in the ovBNST translates into anxiety-like behaviour in the EPM. However, anatomical studies enable us to speculate how a NT-induced decrease of ovBNST activity could affect the HPA axis. The ovBNST has strong GABAergic outputs onto the fusiform nucleus of the BNST (fuBNST) that has direct inhibitory inputs onto the paraventricular nucleus of the hypothalamus (Dong *et al*, 2001). Lesion of the fuBNST attenuates HPA axis response suggesting it enhances PVN activity (Choi *et al*, 2007). As such, a NT-mediated reduction of ovBNST inhibition output to the fuBNST could promote HPA axis excitation and result in a decrease of EPM open arm exploration. Parallel to this, in the PVN, blocking NT receptor during stress counteracts the increase of plasma corticosterone levels (Geisler *et al*, 2006). Additionally, decrease activity in ovBNST inhibitory projections could increase fear/anxiety (CeA), vigilance and arousal (substantia innominata), respiration (parabrachial nucleus) and, defensive response (periaqueductal gray) (Dong *et al*, 2001). At this point however, we cannot discern the exact output of the ovBNST and whether it is affecting local or extrinsic circuitry.

The NT system in different brain areas could be working in concert to stimulate the HPA axis during stress conditions. Future studies should explore whether the magnitude of NT-activation of the HPA axis could possibly correlate with maladaptive vs adaptive behaviour.

Funding and Disclosure

Catherine P. Normandeau reported no biomedical financial interests or potential conflicts of interest and was funded by CIHR Vanier Graduate Scholarship (338319).

Dr. Ana Paula Ventura Silva reported no biomedical financial interests or potential conflicts of interest and was funded by Fundação para a Ciência e Tecnologia (SFRH/BPD/52078/2013).

Dr. Emily R. Hawken reported no biomedical financial interests or potential conflicts of interest and was funded by CIHR Postdoctoral Fellowship (MFE-123712).

Staci Angelis reported no biomedical financial interests or potential conflicts of interest and was funded by a Queen Elizabeth II Graduate Scholarship in Science and Technology.

Dr. Calvin Sjaarda reported no biomedical financial interests or potential conflicts of interest.

Dr. Xudong Liu reported no biomedical financial interests or potential conflicts of interest.

Dr. José Miguel Pêgo reported no biomedical financial interests or potential conflicts of interest.

Dr. Éric C. Dumont reported no biomedical financial interests or potential conflicts of interest and was funded by the Canadian Institute of Health Research (MOP-25953 to ECD).

References

Bessa JM, Mesquita AR, Oliveira M, Pego JM, Cerqueira JJ, Palha JA*, et al* (2009). A trans-dimensional approach to the behavioral aspects of depression. *Front Behav Neurosci* **3**: 1.

Binder EB, Kinkead B, Owens MJ, Nemeroff CB (2001). Neurotensin and dopamine interactions. *Pharmacol Rev* **53**(4): 453-486.

Cerqueira JJ, Mailliet F, Almeida OF, Jay TM, Sousa N (2007). The prefrontal cortex as a key target of the maladaptive response to stress. *J Neurosci* **27**(11): 2781-2787.

Choi DC, Furay AR, Evanson NK, Ostrander MM, Ulrich-Lai YM, Herman JP (2007). Bed nucleus of the stria terminalis subregions differentially regulate hypothalamic-pituitary-adrenal axis activity: implications for the integration of limbic inputs. *J Neurosci* **27**(8): 2025-2034.

Conrad KL, Louderback KM, Gessner CP, Winder DG (2011). Stress-induced alterations in anxiety-like behavior and adaptations in plasticity in the bed nucleus of the stria terminalis. *Physiol Behav* **104**(2): 248-256.

Crestani CC, Alves FH, Correa FM, Guimaraes FS, Joca SR (2010). Acute reversible inactivation of the bed nucleus of stria terminalis induces antidepressant-like effect in the rat forced swimming test. *Behav Brain Funct* **6**: 30.

Crowley NA, Bloodgood DW, Hardaway JA, Kendra AM, McCall JG, Al-Hasani R*, et al* (2016). Dynorphin Controls the Gain of an Amygdalar Anxiety Circuit. *Cell Rep* **14**(12): 2774-2783.

Dabrowska J, Hazra R, Ahern TH, Guo JD, McDonald AJ, Mascagni F*, et al* (2011). Neuroanatomical evidence for reciprocal regulation of the corticotrophin-releasing factor and oxytocin systems in the hypothalamus and the bed nucleus of the stria terminalis of the rat: Implications for balancing stress and affect. *Psychoneuroendocrinology* **36**(9): 1312-1326.

Dabrowska J, Hazra R, Guo JD, Li C, Dewitt S, Xu J*, et al* (2013). Striatal-enriched protein tyrosine phosphatase-STEPs toward understanding chronic stress-induced activation of corticotrophin releasing factor neurons in the rat bed nucleus of the stria terminalis. *Biol Psychiatry* **74**(11): 817-826.

Daniel SE, Rainnie DG (2016). Stress Modulation of Opposing Circuits in the Bed Nucleus of the Stria Terminalis. *Neuropsychopharmacology* **41**(1): 103-125.

Day HE, Curran EJ, Watson SJ, Jr., Akil H (1999). Distinct neurochemical populations in the rat central nucleus of the amygdala and bed nucleus of the stria terminalis: evidence for their selective activation by interleukin-1beta. *J Comp Neurol* **413**(1): 113-128.

Deppermann S, Storchak H, Fallgatter AJ, Ehlis AC (2014). Stress-induced neuroplasticity: (mal)adaptation to adverse life events in patients with PTSD--a critical overview. *Neuroscience* **283**: 166-177.

Deutch AY, Bean AJ, Bissette G, Nemeroff CB, Robbins RJ, Roth RH (1987). Stress-induced alterations in neurotensin, somatostatin and corticotropin-releasing factor in mesotelencephalic dopamine system regions. *Brain Res* **417**(2): 350-354.

Dong HW, Petrovich GD, Watts AG, Swanson LW (2001). Basic organization of projections from the oval and fusiform nuclei of the bed nuclei of the stria terminalis in adult rat brain. *J Comp Neurol* **436**(4): 430-455.

Dumont EC, Williams JT (2004). Noradrenaline Triggers GABAA Inhibition of Bed Nucleus of the Stria Terminalis Neurons Projecting to the Ventral Tegmental Area. *J Neurosci* **24**(38): 8198-8204.

Geisler S, Berod A, Zahm DS, Rostene W (2006). Brain neurotensin, psychostimulants, and stress--emphasis on neuroanatomical substrates. *Peptides* **27**(10): 2364-2384.

Glangetas C, Girard D, Groc L, Marsicano G, Chaouloff F, Georges F (2013). Stress switches cannabinoid type-1 (CB1) receptor-dependent plasticity from LTD to LTP in the bed nucleus of the stria terminalis. *J Neurosci* **33**(50): 19657-19663.

Gosselin P, Laberge B (2003). [Etiological factors of generalized anxiety disorder]. *Encephale* **29**(4 Pt 1): 351-361.

Hammack SE, Mania I, Rainnie DG (2007). Differential expression of intrinsic membrane currents in defined cell types of the anterolateral bed nucleus of the stria terminalis. *J Neurophysiol* **98**(2): 638-656.

Hammen C, Kim EY, Eberhart NK, Brennan PA (2009). Chronic and acute stress and the prediction of major depression in women. *Depress Anxiety* **26**(8): 718-723.

Herman JP (2013). Neural control of chronic stress adaptation. *Front Behav Neurosci* **7**: 61.

Hubert GW, Muly EC (2014). Distribution of AMPA receptor subunit glur1 in the bed nucleus of the stria terminalis and effect of stress. *Synapse* **68**(5): 194-201.

Iremonger KJ, Bains JS (2009). Retrograde opioid signaling regulates glutamatergic transmission in the hypothalamus. *J Neurosci* **29**(22): 7349-7358.

Jassar BS, Harris KH, Ostashewski PM, Jhamandas JH (1999). Ionic mechanisms of action of neurotensin in acutely dissociated neurons from the diagonal band of Broca of the rat. *J Neurophysiol* **81**(1): 234-246.

Ju G, Han ZS (1989a). Coexistence of corticotropin releasing factor and neurotensin within oval nucleus neurons in the bed nuclei of the stria terminalis in the rat. *Neurosci Lett* **99**(3): 246-250.

Ju G, Swanson LW, Simerly RB (1989b). Studies on the cellular architecture of the bed nuclei of the stria terminalis in the rat: II. Chemoarchitecture. *J Comp Neurol* **280**(4): 603-621.

Kash TL, Winder DG (2006). Neuropeptide Y and corticotropin-releasing factor bi-directionally modulate inhibitory synaptic transmission in the bed nucleus of the stria terminalis. *Neuropharmacology* **51**(5): 1013-1022.

Kim SY, Adhikari A, Lee SY, Marshel JH, Kim CK, Mallory CS*, et al* (2013). Diverging neural pathways assemble a behavioural state from separable features in anxiety. *Nature* **496**(7444): 219-223.

Krawczyk M, Georges F, Sharma R, Mason X, Berthet A, Bezard E*, et al* (2011a). Double-dissociation of the catecholaminergic modulation of synaptic transmission in the oval bed nucleus of the stria terminalis. *J Neurophysiol* **105**(1): 145-153.

Krawczyk M, Mason X, DeBacker J, Sharma R, Normandeau CP, Hawken ER*, et al* (2013). D1 dopamine receptor-mediated LTP at GABA synapses encodes motivation to self-administer cocaine in rats. *J Neurosci* **33**(29): 11960-11971.

Krawczyk M, Sharma R, Mason X, Debacker J, Jones AA, Dumont EC (2011b). A switch in the neuromodulatory effects of dopamine in the oval bed nucleus of the stria terminalis associated with cocaine self-administration in rats. *J Neurosci* **31**(24): 8928-8935.

Larriva-Sahd J (2006). Histological and cytological study of the bed nuclei of the stria terminalis in adult rat. II. Oval nucleus: extrinsic inputs, cell types, neuropil, and neuronal modules. *J Comp Neurol* **497**(5): 772-807.

Laszlo K, Toth K, Kertes E, Peczely L, Ollmann T, Lenard L (2010). Effects of neurotensin in amygdaloid spatial learning mechanisms. *Behav Brain Res* **210**(2): 280-283.

Lezak KR, Roman CW, Braas KM, Schutz KC, Falls WA, Schulkin J*, et al* (2014). Regulation of bed nucleus of the stria terminalis PACAP expression by stress and corticosterone. *J Mol Neurosci* **54**(3): 477-484.

Li C, Pleil KE, Stamatakis AM, Busan S, Vong L, Lowell BB*, et al* (2012). Presynaptic inhibition of gamma-aminobutyric acid release in the bed nucleus of the stria terminalis by kappa opioid receptor signaling. *Biol psychiatry* **71**(8): 725-732.

Li J, Song J, Zaytseva YY, Liu Y, Rychahou P, Jiang K*, et al* (2016). An obligatory role for neurotensin in high-fat-diet-induced obesity. *Nature* **533**(7603): 411-415.

Ludwig M, Pittman QJ (2003). Talking back: dendritic neurotransmitter release. *Trends Neurosci* **26**(5): 255-261.

Luttinger D, King RA, Sheppard D, Strupp J, Nemeroff CB, Prange AJ, Jr. (1982). The effect of neurotensin on food consumption in the rat. *Eur J Pharmacol* **81**(3): 499-503.

Mazzone CM, Pati D, Michaelides M, DiBerto J, Fox JH, Tipton G*, et al* (2016). Acute engagement of Gq-mediated signaling in the bed nucleus of the stria terminalis induces anxiety-like behavior. *Mol Psychiatry*.

McElligott ZA, Klug JR, Nobis WP, Patel S, Grueter BA, Kash TL*, et al* (2010). Distinct forms of Gq-receptor-dependent plasticity of excitatory transmission in the BNST are differentially affected by stress. *Proc Natl Acad Sci U S A* **107**(5): 2271-2276.

McElligott ZA, Winder DG (2008). Alpha1-adrenergic receptor-induced heterosynaptic long-term depression in the bed nucleus of the stria terminalis is disrupted in mouse models of affective disorders. *Neuropsychopharmacology* **33**(10): 2313-2323.

Peeters PJ, Fierens FL, van den Wyngaert I, Goehlmann HW, Swagemakers SM, Kass SU*, et al* (2004). Gene expression profiles highlight adaptive brain mechanisms in corticotropin releasing factor overexpressing mice. *Brain Res Mol Brain Res* **129**(1-2): 135-150.

Pego JM, Morgado P, Pinto LG, Cerqueira JJ, Almeida OF, Sousa N (2008). Dissociation of the morphological correlates of stress-induced anxiety and fear. *Eur J Neurosci* **27**(6): 1503-1516.

Poulin JF, Arbour D, Laforest S, Drolet G (2009). Neuroanatomical characterization of endogenous opioids in the bed nucleus of the stria terminalis. *Prog Neuropsychopharmacol Biol Psychiatry* **33**(8): 1356-1365.

Puente N, Elezgarai I, Lafourcade M, Reguero L, Marsicano G, Georges F*, et al* (2010). Localization and function of the cannabinoid CB1 receptor in the anterolateral bed nucleus of the stria terminalis. *PloS one* **5**(1): e8869.

Richard F, Barroso S, Martinez J, Labbe-Jullie C, Kitabgi P (2001). Agonism, inverse agonism, and neutral antagonism at the constitutively active human neurotensin receptor 2. *Mol Pharmacol* **60**(6): 1392-1398.

Saiz Ruiz J, Carrasco Perera JL, Hernanz A (1992). [Plasma neuropeptides in affective and anxiety disorders]. *Arch Neurobiol (Madr)* **55**(1): 1-5.

Shields AD, Wang Q, Winder DG (2009). alpha2A-adrenergic receptors heterosynaptically regulate glutamatergic transmission in the bed nucleus of the stria terminalis. *Neuroscience* **163**(1): 339-351.

Toda H, Boku S, Nakagawa S, Inoue T, Kato A, Takamura N*, et al* (2014). Maternal separation enhances conditioned fear and decreases the mRNA levels of the neurotensin receptor 1 gene with hypermethylation of this gene in the rat amygdala. *PLoS One* **9**(5): e97421.

Vyas A, Bernal S, Chattarji S (2003). Effects of chronic stress on dendritic arborization in the central and extended amygdala. *Brain Res* **965**(1-2): 290-294.

Walker DL, Miles LA, Davis M (2009). Selective participation of the bed nucleus of the stria terminalis and CRF in sustained anxiety-like versus phasic fear-like responses. *Prog Neuropsychopharmacol Biol Psychiatry* **33**(8): 1291-1308.

Woodhams PL, Roberts GW, Polak JM, Crow TJ (1983). Distribution of neuropeptides in the limbic system of the rat: the bed nucleus of the stria terminalis, septum and preoptic area. *Neuroscience* **8**(4): 677-703.

Xiao Z, Cilz NI, Kurada L, Hu B, Yang C, Wada E*, et al* (2014). Activation of neurotensin receptor 1 facilitates neuronal excitability and spatial learning and memory in the entorhinal cortex: beneficial actions in an Alzheimer's disease model. *J Neurosci* **34**(20): 7027-7042.

Figure Legends

Figure 1. Effect of post-synaptic depolarization on $GABA_A$ synaptic transmission in the ovBNST of non-stressed (NS) rats. Effect of post-synaptic activation on the amplitude of electrically-evoked $GABA_A$-IPSCs over time in the ovBNST of NS rats in **(A)** aCSF **(B)** with intracellular concanamycin (5μM) **(C)** with extracellular SR-142948 (10μM) **(D)** with extracellular NBI-27914 **(E)** with extracellular NBI-27914 (1μM) and SR-142948 (10μM). Insets in panels **A-E** show representative ovBNST $GABA_A$-IPSCs before and after post-synaptic activation followed by the proportion of responding neurons. Bar scale: 250 pA and 25 ms. Double arrows represent post-synaptic depolarization (0mV, 100ms at 2Hz, 5 mins) (**F**) Histogram summarizing the proportion of responding neurons to post-synaptic depolarization across different pharmacological treatments. Asterisk; $p<0.05$.

Figure 2. Effect of post-synaptic depolarization on $GABA_A$ synaptic transmission in the ovBNST of chronic unpredictable stress (CUS) exposed rats. Effect of post-synaptic activation on the amplitude of electrically-evoked $GABA_A$-IPSCs over time in the ovBNST of CUS rats in **(A)** aCSF, **(B)** with extracellular SR-142948 (10μM), **(C)** with extracellular NBI-27914 (1μM), **(D)** with extracellular NBI-27914 (1μM) and SR-142948 (10μM). Insets in panels **A-D** show representative ovBNST evoked $GABA_A$-IPSCs before and after post-synaptic activation followed by the proportion of responding neurons. Bar scale: 250 pA and 25 ms. Double arrows represent post-synaptic depolarization (0mV, 100ms at 2Hz, 5 mins) **(E)** Histogram summarizing the proportion of responding neurons to post-synaptic depolarization

across different pharmacological treatments. **(F, G)** Histogram showing fold change in mRNA expression of *Crhr1*, *Crhr2*, *Crh*, *Ntsr1*, *Ntsr2* and *Nts* in CUS compared to NS rats in the dBNST and CeA. Asterisks, $p<0.05$.

Figure 3. Effect of post-synaptic depolarization on AMPA synaptic transmission in the ovBNST of NS rats. Effect of post-synaptic activation on the amplitude of electrically-evoked AMPA-EPSCs over time in the ovBNST of NS rats in **(A)** aCSF and **(B)** with extracellular Naloxone (1 μM). Insets in panels in **A** and **B** show representative ovBNST evoked AMPA-EPSCs before and after post-synaptic activation followed by the proportion of responding neurons. Bar scale: 250 pA and 25 ms. Double arrows represent post-synaptic depolarization (0mV, 100ms at 2Hz, 5 mins) **(C)** Histogram summarizing the proportion of responding neurons to post-synaptic depolarization across different pharmacological treatments. Asterisk; $p<0.05$.

Figure 4. Effect of post-synaptic depolarization on AMPA synaptic transmission in the ovBNST of CUS rats. Effect of post-synaptic activation on the amplitude of electrically-evoked AMPA-EPSCs over time in the ovBNST of CUS rats in **(A)** aCSF and **(B)** with extracellular Naloxone (1μM). Insets in panels **A** and **B** show representative ovBNST evoked AMPA-EPSCs before and after post-synaptic activation followed by the proportion of responding neurons. Bar scale: 250 pA and 25 ms. Double arrows represent post-synaptic depolarization (0mV, 100ms at 2Hz, 5 mins) **(C)** Histogram summarizing the proportion of responding neurons to post-

synaptic depolarization across different pharmacological treatments. Asterisk, $p<0.05$.

Figure 5. Effect of intra-ovBNST NTR pharmacological blockade on elevated plus maze (EPM) and forced swim test (FST) behaviours in NS and CUS rats. **(A)** Experimental timeline. **(B)** Photomicrograph showing a representative accurate bilateral cannula placement. **(C)** Drawing showing all intracranial cannula placements. **(D)** Bar graph representing the percentage of time spent in the EPM open arms (OA) across experimental groups. **(E)** Bar graph representing the number of OA entry across experimental groups. **(F)** Bar graph representing immobility scores in the FST across experimental groups. Sal, saline; SR5, SR 142948 (5 μM); SR 10, SR-142948 (10 μM), Accl./Surg., acclimatation/surgeries; Hist, histology. Asterisks, $p<0.05$.